Available online at www.sciencedirect.com
ScienceDirect
Catalysis Communications 9 (2008) 146–152
CATALYSIS COMMUNICATIONS
www.elsevier.com/locate/catcom

Simple fabrication of thermally stable apertured N-doped TiO_2 microtubes as a highly efficient photocatalyst under visible light irradiation

Jian-hua Xu [a], Wei-Lin Dai [a,*], Jingxia Li [a], Yong Cao [a], Hexing Li [b], Heyong He [a], Kangnian Fan [a]

[a] Department of Chemistry and Shanghai Key Laboratory of Molecular Catalysis and Innovative Materials, Fudan University, Shanghai 200433, PR China
[b] Department of Chemistry, Shanghai Normal University, Shanghai 200234, PR China

Received 21 October 2006; received in revised form 1 May 2007; accepted 22 May 2007
Available online 9 June 2007

Abstract

Apertured N-doped TiO_2 microtubes have been fabricated by simple hydrolysis of titania tetrachloride using ammonia without any external templates. The morphology and microstucture characteristics of apertured N-doped TiO_2 microtubes were characterized by means of the specific surface area (BET), transmission electron microscopy (TEM), scanning electron microscopy (SEM), X-ray photoelectron spectroscopy (XPS), Fourier transformed infrared (FT-IR), UV–visible diffuse reflectance spectra (DRS) and X-ray powder diffraction (XRD). The unique morphology of microtubes and mesoporous microstructure were maintained after a heat treatment at 723 K for 3 h, exhibiting significantly thermal stability. The catalysts exhibited high ultraviolet and visible light photocatalytic activity in degrading phenol and methyl orange.

Keywords: Titanium dioxide; Anatase; Titanium tetrachloride; Nitrogen-doped; Photodegradation

1. Introduction

Semiconductor photocatalysis is an efficient method for the chemical utilization of solar energy. TiO_2, among various photocatalysts, is most frequently employed owing to its cheapness, nontoxicity, and structural stability [1–5]. However, the widespread technological use of TiO_2 is impaired by its wide band gap (ca. 3.2 eV for crystalline anatase phase) which requires the use of UV light during the reaction, thus limiting the possibility of employing solar light in TiO_2 photocatalysis.

Sato et al. reported in 1986 that modification of TiO_2 with the N dopant is a powerful way to extend the adsorption light from UV to visible area, since substitution of the lattice oxygen with nitrogen might narrow the band gap by mixing the N_{1S} and O_{1S} states [6]. Up to now, most N-TiO_2 samples were prepared by treating TiO_2 under NH_3 atmosphere at very high temperature. Besides the energy waste, the treatment at such high temperature usually resulted in the low surface area due to the undesirable sintering of nanocrystallites [7,8]. Hence, the seeking of new facile approaches to the synthesis of N-TiO_2 caught hold of increasingly interesting.

It is also known that hierarchically ordered mesoporous TiO_2 materials may be promising candidates in the field of photocatalysis owing to their large surface area and convenient mass transfer in mesopores in degrading large pollution molecules. However, these TiO_2 materials are traditionally prepared by using surfactant templating in which supramolecular aggregates are considered to direct inorganic deposition across a range of length scales

* Corresponding author. Tel.: +86 21 65643792 6; fax: 86 21 65642978.
E-mail address: wldai@fudan.edu.cn (W.-L. Dai).

1566-7367/$ - see front matter © 2007 Elsevier B.V. All rights reserved.
doi:10.1016/j.catcom.2007.05.043

[9,10]. The organic templates must then be removed by thermal treatment, resulting in high energy consumption, environmental pollution and most important the agglomeration and collapse of pore structure in many cases [11–13]. So most reported mesoporous titania have a low thermal stability. To the best of our knowledge, no hierarchically ordered mesoporous N-TiO_2 material with highly thermal stability has been reported yet without any templates under mild conditions.

In the present work, we use a simple template-free approach to the synthesis of N-TiO_2 photocatalysts with visible light response via a low-temperature precipitation treatment of $TiCl_4$ by ammonia with the presence of glacial acetic acid. The reaction condition is much milder than that of conventional methods. In addition, it is more interesting to find that the N-TiO_2 sample shows a unique apertured microtube structure which has never been reported yet.

2. Experimental

Titanium tetrachloride ($TiCl_4$, analytical reagent grade) was used as titanium precursor of the preparation of the apertured N-TiO_2 microtubes. Commercially available reagents were obtained from Aldrich and used without further purification. In a typical procedure, 25 mL of dilute aqueous solution of $TiCl_4$ (3.0 mol L^{-1}) was carefully added into 150 mL deionized water with gentle stirring in ice-water bath to avoid a drastic hydrolysis of $TiCl_4$ in water at room temperature. Then the solution was heated to 323 K. After that, 4.5 mL of glacial acetic acid and a 35 wt.% solution of ammonia was added dropwise with vigorous stirring until pH 8, then the mixed solution was quickly cooled down to ambient temperature (about 298 K) by rinsed with running water. After aging in the mother liquor for a few days, the resultant slurry was suction-filtered and washed with distilled water until pH 7 and then washed carefully with absolute ethanol for three times. The N-TiO_2 microtube samples were finally obtained after the as-prepared filter residue being vacuum-dried at 353 K for 12 h, followed by calcination at 723 K in flowing air for 3 h. The yield of these microtubes could reach up to about 35%.

The morphology was analyzed by scanning electron microscopy (SEM, Philips XL 30) and transmission electron microscopy (TEM, JEOL-2011, operated at 200 kV). The samples for TEM were prepared by grinding and subsequent dispersing the powder in acetone and applying a drop of very dilute suspension on carbon-coated grids. The textural structures were measured by N_2 adsorption at 77 K in a Micromeritics TriStar ASAP 3000 system. The X-ray powder diffraction (XRD) patterns, obtained on a Bruker D8 Advance X-ray diffractometer using Cu Kα radiation ($\lambda = 1.5418$ Å), were used to identify the phase constitutions in samples and their crystallite size. The accelerating voltage and the applied current were 40 kV and 40 mA, respectively. The crystallite size was calculated from X-ray line broadening analysis by Scherrer equation. Estimation of the content of anatase is based on: $X_A = 1/[1 + 1.265 I_R/I_A] \times 100\%$, where I_A is the (1 0 1) peak intensity of anatase, I_R is the (1 1 0) peak intensity of rutile, and 1.265 is the scattering coefficient. X-ray photoelectron spectroscopy (XPS) measurements were performed on a PHI 5000C ESCA System with Mg Kα source at 14.0 kV and 25 mA, respectively. All the binding energies were referenced to the C1s peak at 284.6 eV of the surface adventitious carbon. All samples were calcined under 723 K for 3 h to eliminate removable nitrogen adsorbent. UV–visible diffuse reflectance spectra (UV–visible DRS) were achieved using a UV–visible spectrophotometer (Shimadzu UV-2450) using $BaSO_4$ as the reference sample. Fourier transformed infrared (FT-IR) characterization was performed on a NEXUS 470 system.

The photocatalytic activities of the N-TiO_2 samples were measured by the degradation of phenol and methyl orange in an aqueous solution with concentration at 0.060 and 0.020 g L^{-1}, respectively. Flowing air was bubbled into the solution before irradiation for 30 min in order to establish the adsorption equilibrium and throughout the experiment. Four 8 W lamps with various wavelength (254, 365, 420 nm, respectively) were used as ultraviolet and visible light source. 0.050 g of photocatalyst was suspended in a 50 mL aqueous solution of organic reactants. The temperature was controlled at 298 ± 1 K during the overall degradation process. The concentrations of which were measured with a UV–visible spectrophotometer (Shimadzu UV-2450). Millipore discs were used to separate the catalysts before the analysis. The measurements were repeated for each catalyst and the experimental error was found to be within $\pm 3\%$.

3. Results and discussion

The SEM image displayed in Fig. 1a shows that the unique morphology of the apertured N-TiO_2 microtubes can be preserved well after calcination. The average diameter of each microtube is about 10 μm with the shell thickness about 1 μm. An expanded view in inset (a) gives the array of ventages exhibited regularly on the shell of the microtubes, and the average diameter of each hole is about 1 μm with the interval of ca. 4 μm. TEM analyses were performed to examine the nanocrystallites that make up the microtubes. Fig. 1b presents the nanocrystalline nature of anatase TiO_2. It is found that the size of anatase nanocrystallites is approximately 10 nm. High resolution TEM (top inset of Fig. 1b), confirmed that the sample were comprised of connected crystalline titania nanoparticles (the ovals in the figure), with a lattice spacing consistent with the anatase phase (0.352 nm), giving evidence the polycrystalline nature of N-TiO_2 sample which fit well with the XRD patterns. Besides, we can directly examine the average crystallite size of TiO_2 nanoparticles which is consistent well with that calculated from the XRD data (see Fig. 2), calculate the average pore diameter and compare with the result

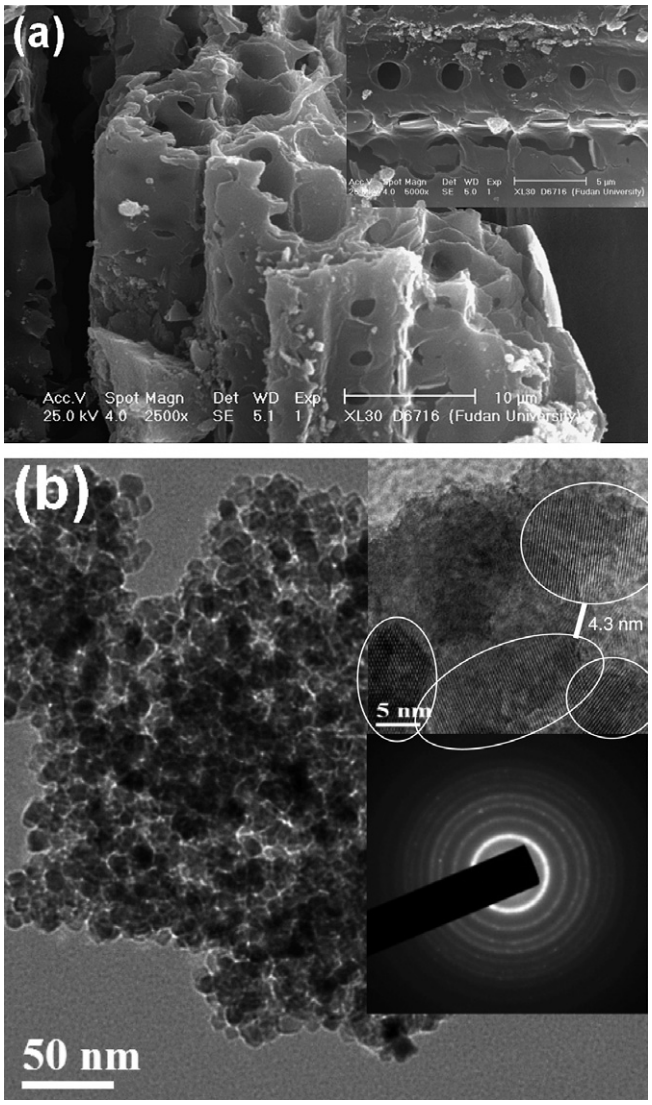

Fig. 1. SEM (a) and TEM (b) images of the mesoporous apertured N-doped TiO_2 microtubes after calcination at 723 K. The top inset of (b) was its HRTEM figure. The SAED image in inset (b) displaying the crystalline nature (anatase) of the titania nanoparticles that make up the apertured microtubes.

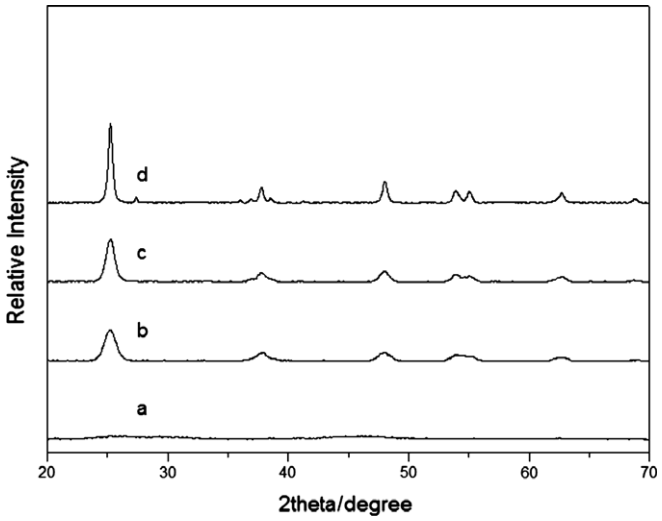

Fig. 2. XRD patterns of mesoporous N-TiO_2 samples. (a) As-prepared, (b) sample calcined for 3 h under 623 K, (c) 723 K and (d) 823 K.

from N_2 adsorption characterization (see Fig. 4). The selected-area electron diffraction (SAED) characteristics (middle inset of Fig. 1b) further confirmed that the titania nanoparticles showed crystalline anatase phase. Such high anatase crystallinity in the mesoporous TiO_2 was highly desirable in photocatalysis [14].

The formation of hierarchical porous shapes was usually explained by facet selectivity of the templates during the crystallite growth of the synthesis, while no template is used in our present work for the synthesis and the formation of apertured titania microtubes happens during the processing. There might be another mechanism for the formation of TiO_2 microtubes. In order to examine the processing parameters that control the morphology and structural properties of the TiO_2 microtubes, factors affecting the hydrolysis process including the amount of acetic acid additive, $TiCl_4$, reaction temperature, aging temperature and time were investigated. By varying these parameters, we found that the preparation parameters were of vital importance in the final formation of titania. It was found that a higher precipitating temperature and aging at ambient temperature may favor the formation of TiO_2 microtubes with well-developed mesoporosity. The use of acetic acid as a dispersing agent was of crucial importance in the preparation of titania with apertured microtube morphology. The essential role of acetic acid in promoting the formation of mesoporous TiO_2 microtubes might be understood by taking into account the behavior as a ligand and the modification of the polymeric structure at a molecular level, which promoted the emergence of polymeric structures [15].

It is known that acetic acid is a rather weak electrolyte with a low degree of dissociation, so here it is a good buffer, which can keep a stable pH range in this reaction system. The suitable pH value could effectively control the hydrolysis rate of $TiCl_4$ in the initial reaction stage. There are lone pair electrons on nitrogen atoms of ammonia, which provides the possibility that $TiCl_4$ can combine with the ammonia to form a complex. During the hydrolysis process, the titania nanoparticles begin to form and tend to aggregate each other. The presence of glacial acetic acid can kinetically control the growth rate of titania nanoparticles and their assembly into microtubes [16]. In addition, the assemble process become slower and halt while the concentration of Ti source decreases, so the microtubes were not finally formed and some ventages were remained in the wall. To confirm this mechanism of the formation of the apertured TiO_2 microtubes, various concentration of $TiCl_4$ was tested and we found more $TiCl_4$ would lead to TiO_2 microtubes without ventages and less $TiCl_4$ would result in twist-like helix microbelts.

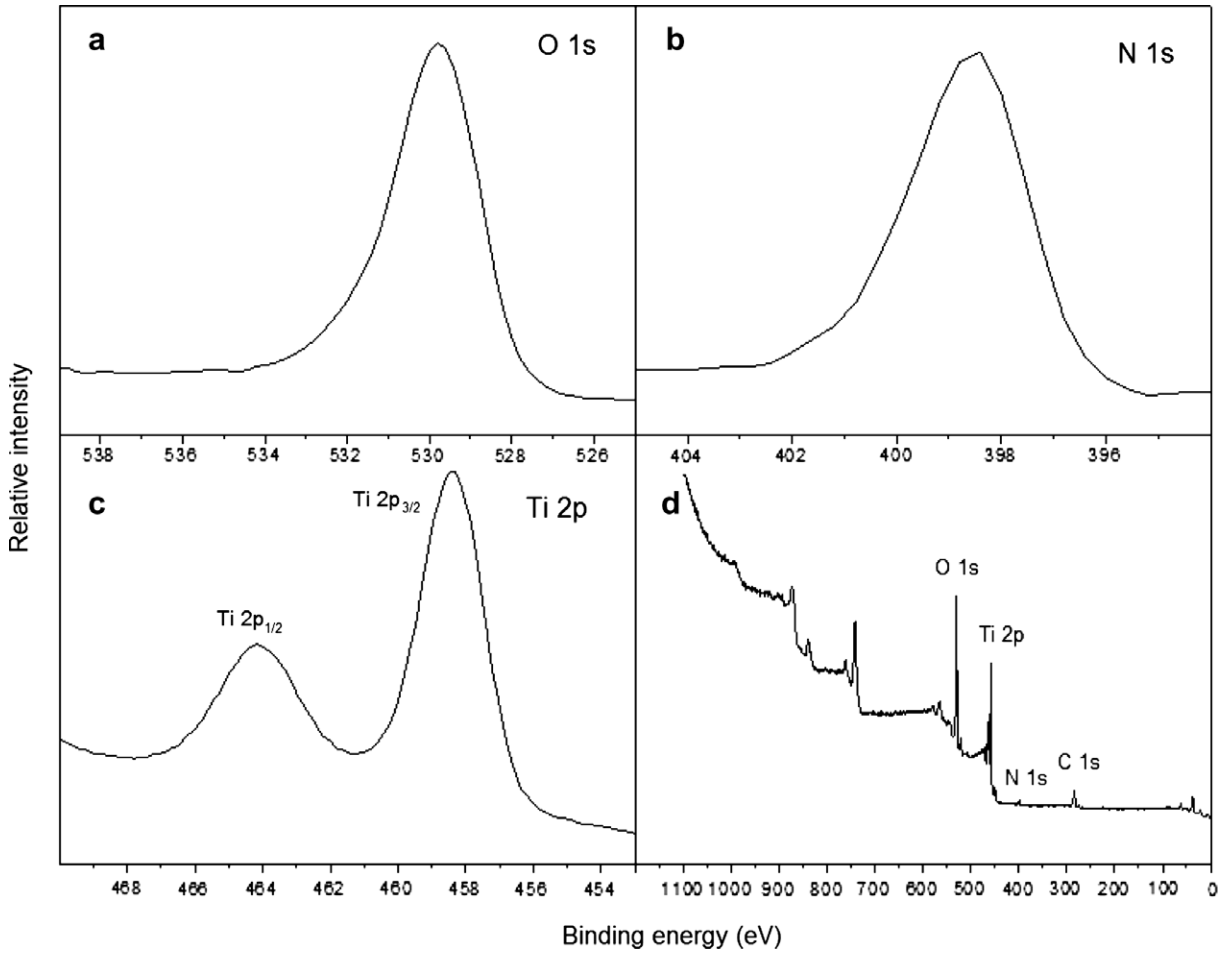

Fig. 3. (a) XPS spectra of the O_{1s}, (b) N_{1s}, (c) Ti_{2p} and (d) full regions for the 723 K calcined N-TiO_2 microtubes. The nitrogen percentage of which is ca. 2.9% (atomic ratio).

The well crystallization and high stability of titania microtubes can be explained by the XPS spectra (Fig. 3). There are two kinds of N species in N-doped TiO_2 materials, the N bonded with Ti and molecularly chemisorbed NH_3. After a thermal treatment at 723 K for 3 h, almost all of the chemisorbed NH_3 can be eliminated [17]. According to the XPS result, the nitrogen percent in the N-TiO_2 remains 2.9% after calcination, which can prove the formation of N–Ti–O bond [8,18]. The formation of these bonds can inhibit the integratation of titania particles and enhance the crystallization degree of anatase phase during calcination process. Moreover this unique apertured microtube N-TiO_2 prepared by ammonia treatment exhibited an outstanding thermal stability to at least 773 K, whereas the ordinary mesoporous titania samples completely collapse at a calcination temperature at 623 K [19].

The porosity of the titania materials has been investigated using nitrogen adsorption–desorption isotherms. Fig. 4 gives the nitrogen adsorption–desorption isotherm of the as-prepared sample, it exhibits a type IV isotherm with an inflection of nitrogen adsorbed volume at $P/P_0 = 0.45$ (type H2 hysteresis loop), being representative

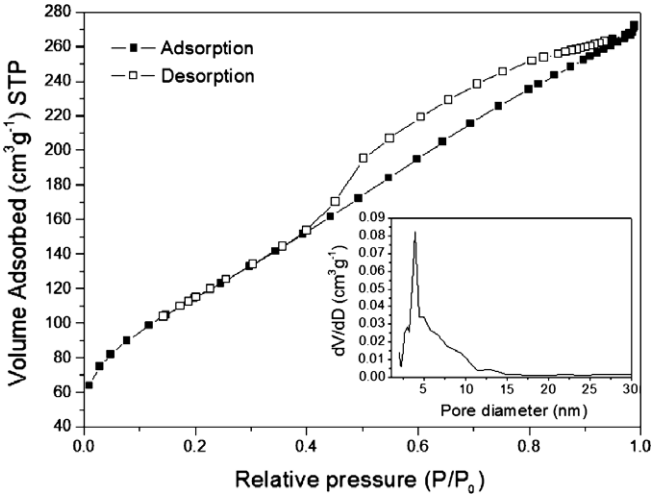

Fig. 4. Nitrogen adsorption/desorption isotherms and the corresponding pore size distribution curves (inset) for the as-prepared N-TiO_2 sample.

of well-developed mesoporosity in the titania samples. A typical value for the specific surface area using the BET method is 419 $m^2\,g^{-1}$, much higher than the reported TiO_2 obtained by conventional method [20]. The inset in

Fig. 4 shows the pore size distribution (PSD) plots estimated using the BJH (Barrett–Joyner–Halenda) equation from the desorption branch of the isotherm. The PSD measurements show that the titania sample had pronounced mesoporosity of a very narrow pore size distribution with an average pore diameter at ca. 4.3 nm. The mesopores of N-doped TiO_2 microtubes was located in the interparticle of nanocrystallites. According to the XRD data, the size of TiO_2 nanocrystallites estimated by Scherrer equation were about 10 nm, also we can find the size of nanocrystallites was nearly the same from the TEM image. These nanocrystallites were accumulated and suggested to form mesopores between each other. The average accumulative pore diameter was ca. 4.3 nm, which was shown in the HRTEM figure (top inset of Fig. 1b). These results illustrate that the doping with nitrogen does not change the textural properties of TiO_2 significantly. The nitrogen species are embedded in the TiO_2 network of the mesoporous pore walls, and the pore channels remain open. Such open mesoporous architecture, large surface area and 3D-connected pore system, play an important role in catalyst design for its ability to improve the molecular transport of reactants and products [21] (see Table 1).

The UV–visible DRS spectra of the mesoporous N-TiO_2 samples are shown in Fig. 5. The optical band edge of the mesoporous N-TiO_2 exhibits a remarkable red-shift with respect to that of pure TiO_2 (P25). This can be assigned to the substitution of crystal lattice O to N species, which is consistent with the XPS results. The enhanced ability to absorb visible light makes this mesoporous N-TiO_2 an effective photocatalyst for solar-driven applications.

FT-IR spectrum of N-TiO_2 samples was shown in Fig. 6. The FT-IR characterization can further confirm the substitution of crystal lattice O to N species and the formation of N–Ti–O bond. The absorption peaks at 3400, 2930 and 2850 cm^{-1} were assigned to the OH species [22]. The absorption peak at 1630 cm^{-1} belongs to the Ti–O structure, 1380 cm^{-1} corresponding to the surface adsorbed NH_3 molecules [23]. The peaks at 1450, 1230, and 1090 cm^{-1} could be attributed to the nitrogen atoms embedded in the TiO_2 network [19,24]. These results clearly demonstrated that the hydrolysis of $TiCl_4$ in ammonia solution under this reaction conditions resulted in not only the chemisorption of NH_3 molecules on the TiO_2 surface but also the nitridation of the TiO_2 lattice. The nitridation occurred by replacing the oxygen atom in the TiO_2 with the nitrogen atom in the NH_3 molecule, resulting in the formation of the O–Ti–N and the N–Ti–N as well the OH species. The Raman characterization was also performed and besides the three main peak attributed to anatase TiO_2, a weak peak at 570 cm^{-1} belonged to TiO_xN_{2-x} was also found, which can further confirm the existence of N–Ti–O bond [18].

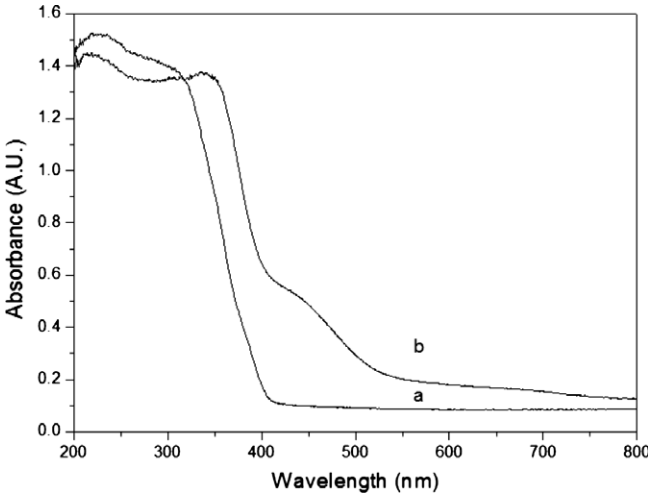

Fig. 5. UV–visible diffuse reflectance spectra of (a) Degussa P25 and (b) 723 K calcined N-TiO_2.

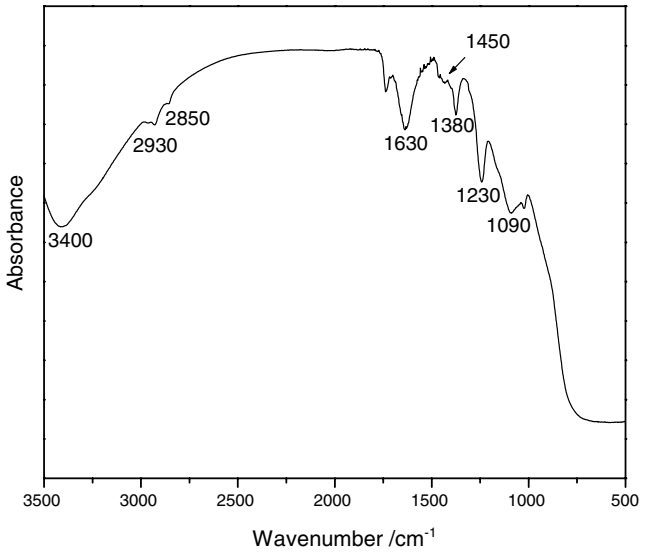

Fig. 6. FT-IR spectra of the as-prepared mesoporous apertured N-doped TiO_2 microtubes.

Table 1
The textural properties of the mesoporous N-TiO_2 samples as a function of calcination temperature

Calcination temperature (K)	S_{BET} ($m^2\ g^{-1}$)	Pore volume ($cm^3\ g^{-1}$)	Average pore diameter (nm)	Anatase (%)	Rutile (%)	Anatase (nm)	Rutile (nm)
As-synthesized	419	0.56	4.3	Amorphous	Amorphous	–	–
623	166	0.44	7.4	100	0	7.0	–
723	122	0.34	9.0	100	0	9.9	–
823	49	0.16	9.0	92	8	20	33
P25	51	0.16	16	77	23	21	24

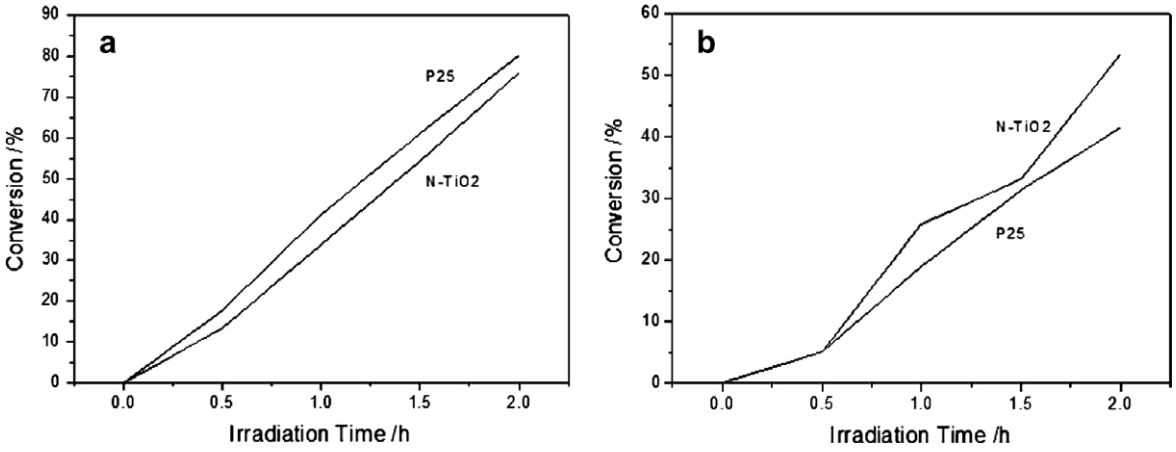

Fig. 7. Photocatalytic activity of N-TiO_2 microtubes: degradation of phenol under ultraviolet irradiation. (a) 254 nm and (b) 365 nm.

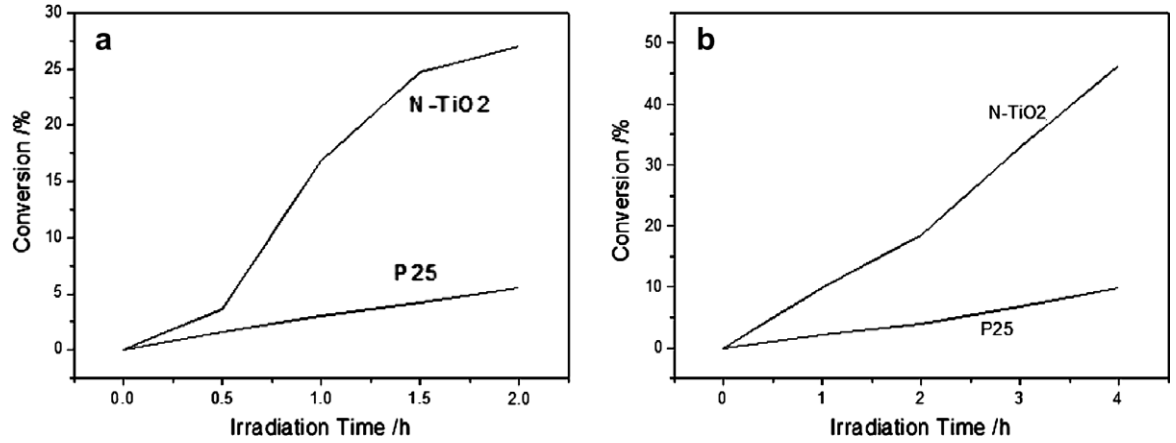

Fig. 8. Photocatalytic activity of N-TiO_2 microtubes: degradation of phenol and methyl orange under visible light (>420 nm) irradiation. (a) Phenol and (b) methyl orange.

To evaluate and compare the photocatalytic activity of the mesoporous N-TiO_2 microtubes, the reactions of phenol and methyl orange degradation were performed as photoreaction probes under UV and visible irradiation, respectively. Results of the photocatalytic evaluation are summarized in Figs. 7 and 8. The commercial catalyst Degussa P25 is a little more effective than N-TiO_2 microtubes under 254 nm irradiation, however, the latter demonstrates a comparatively higher reaction rate under 365 nm irradiation. This was because the differences of absorbing capacity of UV light, while under 254 nm UV irradiation, the absorbance of P25 is a little more than N-TiO_2 samples (see Fig. 5), meaning that P25 can absorb more UV radiation than N-TiO_2. While under 365 nm UV irradiation, the absorbance of N-TiO_2 is far more than that of P25 owing to its significant red shift. This is the main reason why these two catalysts show opposite performance under various wavelength of light in UV range. In the visible light region (>420 nm), the N-TiO_2 microtubes keep relativity high performance while P25 has nearly no activity at all. The expanded photoactivity under visible light is due to the nitrogen doping according to the common accepted opinions. The excellent photocatalytic activity of the N-TiO_2 samples could be attributed to the well-crystalline anatase phase which facilitates the transfer of photo-induced holes from bulk to surface for degradation of organic compounds and also effectively inhibits the recombination between the photo-induced holes and electrons which may enhance the quantum yield [25]. The photocatalytic performance is also related to the mesoporous microstructure of the N-TiO_2 samples with large BET surface areas and a 3D-connected pore system which can help to concentrate the reactant molecules for the photoreactions and the photos might be scattered in between the nanosized TiO_2 particles [26].

4. Conclusions

In summary, we have demonstrated a facile and template-free method for the fabrications of apertured N-TiO_2 microtubes with remarkably thermal stability. The new photocatalysts show high visible light photocatalytic activity on the degradation of phenol and methyl orange owing to their large specific surface area, surface permeability

and well anatase crystallization. The doped nitrogen species play a key role in expanding the photoactivity to visible light region and improving the anatase crystallization and thermal stability. Further work for the examination of the formation mechanism of these apertured N-TiO_2 samples is being under way.

Acknowledgements

We thank the Major State Basic Resource Development Program (Grant No. 2003CB 615807), NSFC (Project 20407006, 20573024) and the Natural Science Foundation of Shanghai Science and Technology Committee (06JC14004) for financial support.

References

[1] A.L. Linsebigler, G.Q. Lu, J.T. Yates, Chem. Rev. 95 (1995) 735.
[2] J.C. Yu, J.G. Yu, W.K. Ho, Z.T. Jiang, L.Z. Zhang, Chem. Mater. 14 (2002) 3808.
[3] C. Kormann, D.W. Bahnemann, M.R. Hoffmann, J. Phys. Chem. 92 (1988) 5196.
[4] S. Klosek, D. Raftery, J. Phys. Chem. B 105 (2001) 2815.
[5] S. Quadawi, S.R. Salman, J. Photochem. Photobiol. A 48 (2002) 161.
[6] S. Sato, Chem. Phys. Lett. 123 (1986) 126.
[7] H. Irie, Y. Watanabe, K. Hashimoto, J. Phys. Chem. B 107 (2003) 5483.
[8] C. Burda, Y.B. Lou, X.B. Chen, A.C.S. Samia, J. Stout, J.L. Gole, Nano Lett. 3 (2003) 1049.
[9] A. Leonard, J.L. Blin, B.L. Su, Chem. Commun. 20 (2003) 2568.
[10] W.H. Deng, M.W. Toepke, B.H. Shanks, Adv. Funct. Mater. 13 (2003) 61.
[11] C.C. Wang, J.Y. Ying, Chem. Mater. 11 (1999) 3113.
[12] C. Su, B.Y. Hong, C.M. Tseng, Catal. Today 96 (2004) 119.
[13] K. Hashimoto, K. Wasada, N. Toukai, H. Kominami, Y. Kera, J. Photochem. Photobiol. A: Chem. 136 (2000) 103.
[14] M.R. Hoffmann, S.T. Martin, W.Y. Choi, D.W. Bahnemann, Chem. Rev. 95 (1995) 69.
[15] M.T. Tsai, J. Non-Cryst. Solids 298 (2002) 116.
[16] R. Asahi, T. Morikawa, T. Ohwaki, K. Aoki, Y. Taga, Science 293 (2001) 269.
[17] J.Y. Gong, S.H. Yu, H.S. Qian, L.B. Luo, X.M. Liu, Chem. Mater. 18 (2006) 2012.
[18] J.L. Gole, J.D. Stout, C. Burda, Y.B. Lou, X.B. Chen, J. Phys. Chem. B 108 (2004) 1230.
[19] H.X. Li, J.X. Li, Y.I. Huo, J. Phys. Chem. B 110 (2006) 1559.
[20] G.Q. Guo, J.K. Whitesell, M.A. Fox, J. Phys. Chem. B 109 (2005) 18781.
[21] J.C. Yu, G.S. Li, X.C. Wang, X.L. Hu, C.W. Leung, Z.D. Zhang, Chem. Commun. 25 (2006) 2717.
[22] M.S.K. Kamal, I.Z.J. Mohamed, Powder Technol. 92 (1997) 233.
[23] L.A. Nalo, C.C. Cerrlos, C.J. Real, Surf. Interface Anal. 24 (1996) 355.
[24] S. Shanmugasundaram, J. Marcin, K.J. Horst, Phys. Chem. B 108 (2004) 19384.
[25] H.X. Li, G.S. Li, J. Zhu, Y. Wan, J. Mol. Catal. A: Chem. 226 (2005) 93.
[26] H. Wang, Y. Wu, B.Q. Xu, Appl. Catal. B: Environ. 59 (2005) 139.